


Article

Investigating the Out-of-Plane Bending Stiffness Properties in Hybrid Species Diagonal-Cross-Laminated Timber Panels

Shaghayegh Kurzinski ^{1,*} and Paul L. Crovella ² 
¹ School of Engineering, Computing and Construction Management, Roger Williams University, Bristol, RI 02809, USA

² Department of Sustainable Resources Management, College of Environmental Science and Forestry, State University of New York, Syracuse, NY 13210, USA; plcrovella@esf.edu

* Correspondence: skurzinski@rwu.edu

Abstract: Since the introduction of Cross-laminated Timber (CLT) in Austria in the early 1990s, the adoption of this 90°-crosswise-laminated product has seen exponential growth worldwide. Compared to traditional laminated timber products (e.g., glulam), CLT provides improved dimensional stability but with reduced out-of-plane bending stiffness. To improve the bending stiffness, while maintaining relative dimensional stability, a modified orientation of the inner layers in a diagonal direction can be used. This novel product is Diagonal-Cross-laminated Timber (DCLT), a composite timber product, consisting of inner layers which are rotated at different angle-ply orientations between 0 and 90 degrees to the outer layers. To properly model the out-of-plane bending behavior of the DCLT, analytical models and finite element analysis (FEA) were used, and the results were validated by four-point bending tests performed on DCLT panels with angle-ply orientations of 10°, 20°, 40°, 70°, and a conventional CLT 90° panel. The results indicate that DCLT panels with angle-ply cross layers have a structural advantage in out-of-plane bending over traditional CLT (90°) panels. The apparent bending stiffness from DCLT 90° to DCLT ± 10° has an increase of 33%, 24%, and 35%, respectively, regarding the assessed methods of experimental, theoretical, and FEM modeling. Using these panels would allow for increased spans or load-carrying capacity for a given panel span-to-depth ratio. The development of DCLT and its introduction to the industry not only could enable the use of lower-quality timber that would not otherwise satisfy structural requirements for CLT but also could help reduce the fabrication cost of CLT due to utilizing lower amounts of fiber.

Keywords: Cross-laminated Timber (CLT); grain orientation; Hankinson's formula; Diagonal-Cross-laminated Timber (DCLT); bending stiffness



Citation: Kurzinski, S.; Crovella, P.L. Investigating the Out-of-Plane Bending Stiffness Properties in Hybrid Species Diagonal-Cross-Laminated Timber Panels. *Appl. Sci.* **2024**, *14*, 2718. <https://doi.org/10.3390/app14072718>

Academic Editors: Almudena Majano Majano, Antonio José Lara Bocanegra and Francisco Arriaga

Received: 2 February 2024

Revised: 12 March 2024

Accepted: 17 March 2024

Published: 24 March 2024



Copyright: © 2024 by the authors. Licensee MDPI, Basel, Switzerland. This article is an open access article distributed under the terms and conditions of the Creative Commons Attribution (CC BY) license (<https://creativecommons.org/licenses/by/4.0/>).

1. Introduction

Wood, a natural orthotropic material, has unique properties in different grain directions of the three mutually perpendicular axes: longitudinal, radial, and tangential (as shown in Figure 1). The longitudinal axis L is parallel to the grain, the radial axis R is normal to the growth rings (perpendicular to the grain in the radial direction), and the tangential axis T is perpendicular to the grain but tangent to the growth rings. The strength and stiffness properties of wood in the grain direction are much higher than the strength and stiffness properties perpendicular to the grain direction. In addition to the mechanical properties, given its hygroscopic nature, wood dimensional changes (i.e., the shrinkage and swelling) occur in each direction and vary with moisture content (MC%). This property of wood is referred to as dimensional stability. The dimensional stability affects how a final timber product will distort in service. The percent shrinkage and swelling of wood are greatest in the tangential direction, less in the radial direction, and least in the longitudinal direction; the latter changes are mostly negligible.

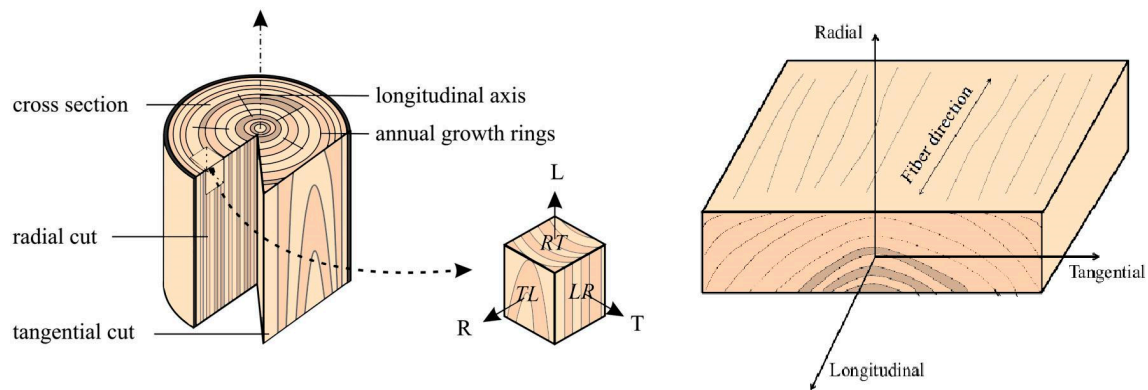


Figure 1. Three perpendicular axes of wood grain orientation.

The natural properties of wood have been the basis for innovations in mass timber products such as Glued-laminated Timber (GLT) and Cross-laminated Timber (CLT). GLT includes layers of timber boards glued together parallel in one major load-bearing direction (0°); CLT consists of crosswise orientated layers, where the layers are orientated perpendicular to each other, providing one major (0°) and one minor (90°) load-bearing direction for out-of-plane bending [1]. The cross layers of CLT help to minimize the overall shrinkage and swelling of the structural panel. Thus, CLT panels show higher dimensional stability compared to GLT beams. For bending out-of-plane, CLT's cross layers are responsible for the panel's bidirectional strength and work to distribute the load in the minor direction as well. However, the cross layers have lower stiffness and strength (in the major axis direction), leading to a greater panel deflection than with GLT. Recognizing these relative advantages and limitations of GLT and CLT, an optimized/modified orientation of the inner layers in a diagonal direction could be developed to improve the out-of-plane bending stiffness while maintaining structural and dimensional stability.

The product created with inner layers at varying angles is called Diagonal-Cross-laminated Timber (DCLT). DCLT can be seen as a standard counterpart to CLT, offering improved mechanical properties using the same panel thicknesses while using less fiber, resulting in lower fabrication and material cost. CLT is a balanced and symmetric laminate since the material properties, the thickness of its layers, and the orientation of its plies are symmetric about the midplane [2]. However, DCLT can be introduced as a balanced and antisymmetric laminate to improve the overall stiffness. This means that in DCLT panels, the plies with the same thickness are a mirror image of the geometrical midplane. Therefore, for each $+\alpha$ angle-ply laminate in the panel, there is an equally thick $-\alpha$ angle-ply laminate as well. Figure 2 illustrates the configurations of GLT, DCLT, and CLT to show how DCLT lay-up can be orientated compared to GLT and CLT products.

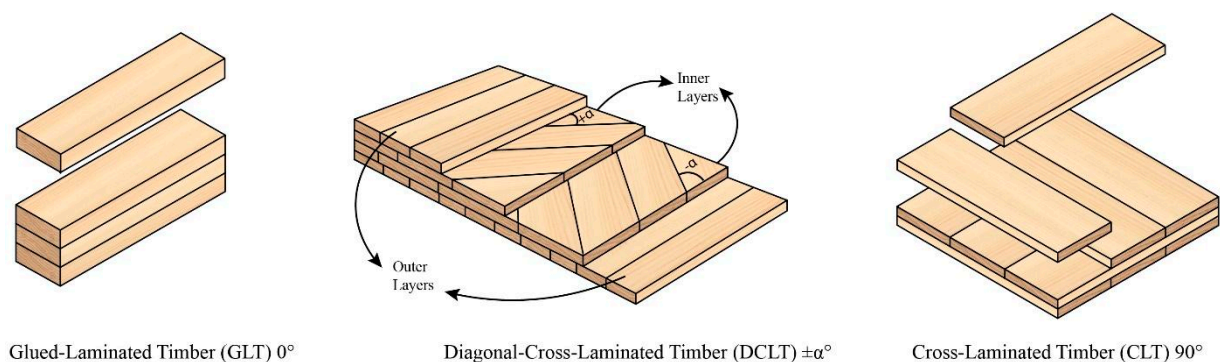


Figure 2. GLT, DCLT, and CLT lay-up configurations [3].

Several studies have been conducted to study the potential relationship between the grain orientation of DCLT's inner lamina and the panel's bending and shear stiffness

properties. Buck et al. [4] investigated the difference between bending stiffness in conventional CLT panels and DCLT panels with inner layers of 45° grain orientation. They tested two groups of 20 five-layered panels, with orientations of $0^\circ-90^\circ-0^\circ-90^\circ-0^\circ$ and $0^\circ-45^\circ-0^\circ-45^\circ-0^\circ$ under four-point bending in the main load-carrying direction in a flat-wise panel lay-up. Their evaluated results confirmed that the DCLT $\pm 45^\circ$ bending strength and the apparent stiffness (EI_{app}) increased, respectively, by 35% and 15% over the conventional CLT panels with 90° layers. EI_{app} is defined as the apparent bending stiffness of the panel in the span direction including both bending and shear deformation, while the EI_{eff} of the panel refers to the effective bending stiffness in the span direction. In another study, these researchers [5] investigated the mechanics of the diagonally and conventionally layered CLT by a digital image correlation (DIC) technique and a destructive four-point bending test on samples with the conventional 90° and $\pm 45^\circ$ alternating inner layers. DIC evaluations of 100 CLT panel layers showed that a considerable part of the stiffness of conventional CLT is reduced by the shear resistance of transverse layers. The overall experimental results showed the shear strain in CLT $\pm 45^\circ$ to be 60% lower than in CLT 90° . The reduced strain in the transverse layers contributes to a stiffer panel and therefore suggests the use of CLT panels with a $\pm 45^\circ$ layered configuration to be a more efficient material to use for timber engineering construction. Their results also showed that utilizing the lower-grade material for the transverse diagonal layers increased the yield values due to the increased stiffness properties of the overall product.

Other researchers have shown interest in studying both the shear and bending performance of DCLT panels with different angle-ply orientations. Bahmanzad et al. [6] performed research on three-ply DCLT panels fabricated from eastern hemlock. The inner layer had grain orientations of 30° , 45° , 60° , and CLT (90°) relative to the main load-bearing direction. Their results of the short-span three-point bending test showed higher shear and bending properties for the DCLT 30° panels, followed by successively lower values for the DCLT 45° , 60° , and CLT (90°) panels. The EI_{app} from their experimental short-span three-point bending results showed an increase of 174%, 112%, and 61%, respectively, for DCLT 30° , DCLT 45° , and DCLT 60° , compared to CLT 90° .

Also, Arnold et al. [2] investigated the load-bearing behavior and efficiency of DCLT under a biaxial bending configuration experimentally and theoretically. They tested seven replicas of CLT and DCLT $\pm 30^\circ$ and $\pm 45^\circ$ panels with different thicknesses. Their evaluation included an evaluation of the increase in the torsional stiffness of DCLT panels compared to conventional CLT panels. They tested an applied parametric numerical model to evaluate the influence of the layer arrangement as well as the width and thickness of the laminations on the torsional stiffness. They also designed an analytical model for finding the torsional stiffness of the panels using two methods: the Kirchhoff–Love and Reissner–Mindlin equations. Their results showed a considerable increase in the torsional stiffness of DCLT panels compared to conventional Cross-laminated Timber panels. Their results confirmed that DCLT could improve biaxial bending stiffness. Therefore, it could be an alternative option to CLT for floor systems governed by serviceability limit states such as deflections or vibrations.

To determine wood properties at an angle to one of the principal axes, Hankinson's criterion is the most common method. Over time, researchers have proposed modifications to the base formula [7]; however, recent studies have confirmed the validity of fit to the experimental data for the original formula. For instance, Bahmanzad et al. [8] studied Hankinson's formula to determine its effectiveness in predicting shear moduli and strength based on grain orientation. The shear stiffness and strength results from the short-span bending tests on three-ply CLT and DCLT panels appeared to fit the data fairly well. Another study regarding the impact of grain orientation on the mechanical properties of DCLT was conducted by Franzoni et al. [9]. They developed a 3D FEM DCLT model with four configurations having the same total thickness but different spans and the mid-layers of the panels orienting from 0° to 90° with an increment of 10° . Their findings confirmed that the failure load and the deflection are functions of grain orientation. Their results

state that the effect on bending stiffness of rotating the grain orientation becomes more significant for DCLT panels with shorter span-to-depth ratios.

This study continues the investigation on the effectiveness of orienting the inner layer of CLT products at another angle rather than the conventional 90° on the overall panel stiffness. This work focuses on the apparent bending stiffness of DCLT panels with various grain orientations in two asymmetric inner layers featuring a feasible lay-up for the future manufacturing of DCLT. In this study, three approaches were used: a theoretical approach, experimental testing, and FEM modeling. For this work, twelve four-ply DCLT $\pm\alpha$ panels and one four-ply CLT panel were fabricated from a local hardwood species, black locust (*Robinia pseudoacacia*), for the parallel (0°) top and bottom layers, and a local softwood species, eastern white pine (*Pinus strobus*), was used for the two diagonal ($\pm\alpha^\circ$) inner layers. Before the experiment, an analytical model was developed using Hankinson's criterion with the shear analogy approach to predict the bending performance of each set of DCLT panels. The shear analogy method proposed by Kreuzinger [10], and used in the US CLT Handbook [11], gives the composite bending and shear stiffness (EI_{eff} , GA_{eff} , and EI_{app}) of the CLT panels using the values of the elastic and shear moduli parallel and perpendicular to the grain (E_0 , E_{90} , G_{90}) of the species in each layer [12]. The bending stiffness properties of the DCLT and CLT panels from this theory were then compared to the experimental results from the four-point bending test. The finite element analysis also simulated the four-point bending test, and the results were compared with the results of the shear analogy method and experimental tests. This study provides methods of predicting the bending stiffness of DCLT and CLT panels with the available or measured elastic modulus parallel to the grain of the species used in the panel fabrication. These methods of prediction could help utilize and introduce non-standard species for the fabrication of these products.

2. Materials and Methodology

2.1. Theoretical Investigations

Initial investigations were conducted on predicting the bending stiffness of DCLT panels with different grain orientation angles and species. An analytical model was developed by applying Hankinson's formula in the shear analogy approach. Hankinson's formula (Equations (1) and (2)) was used to find the axial and shear stiffness values of the angle-ply inner layers, and the final panel stiffness (EI_{app}) was found using the shear analogy approach (Equations (3)–(5)),

$$E_\alpha = \frac{E_0 \times E_{90}}{E_0 \times \alpha + E_{90} \times \alpha} \quad (1)$$

$$G_\alpha = \frac{G_0 \times G_{90}}{G_0 \times \alpha + G_{90} \times \alpha} \quad (2)$$

where α is the angle of the grain orientation of the main axis, E_α is the modulus of elasticity in the major strength direction of the diagonal layer, and E_0 and E_{90} are the moduli of elasticity parallel and perpendicular to the grain. G_α is the shear modulus of the diagonal layer in the span direction, and G_0 and G_{90} are the shear moduli parallel and perpendicular to the grain,

$$EI_{eff} = \sum_{i=1}^n E_i \times b_i \times \frac{h_i^3}{12} + \sum_{i=1}^n E_i \times A_i \times z_i^2 \quad (3)$$

where i is the individual layer of the panel, EI_{eff} is the effective bending stiffness in the span direction, E_i is the modulus of elasticity of the individual layer that can be E_0 for outer layers and E_α for inner layers, b_i is the width of the effective cross-section, h_i is the height

of the individual layer, A_i is the area of the effective cross-section, and z_i is the distance of the neutral axis of the individual layer from the neutral axis of the panel,

$$GA_{eff} = \frac{a^2}{\left[\left(\frac{h_i}{2 \times G_i \times b} \right) + \left(\sum_{i=2}^{n-1} \frac{h_i}{G_i \times b_i} \right) + \left(\frac{h_n}{2 \times G_n \times b} \right) \right]} \quad (4)$$

where, GA_{eff} is the effective shear stiffness in the span direction, a is the distance between the neutral axis of the outer layers, b_i is the width of the effective cross-section, h_i is the height of the individual layer, and G_i is the shear modulus of the individual layer that can be G_0 for outer layers and G_α for inner layers,

$$EI_{app} = \frac{EI_{eff}}{1 + \frac{K_s EI_{eff}}{GA_{eff} \times (l)^2}} \quad (5)$$

where, EI_{app} is the apparent bending stiffness in the span direction including both bending and shear deformation, EI_{eff} is the effective bending stiffness in the span direction using the shear analogy method, GA_{eff} is the effective shear stiffness in the span direction using the shear analogy method, K_s is a factor based on the ratio of deflection due to bending to deflection due to shear (12.96 for four-point loading [13]), and l is the length of the span.

Initially, lay-up alternatives for the hardwood and softwood species selection were assumed. Due to the higher rate of shrinkage/swelling of the hardwood species, black locust, the optimal lay-up was assumed to be a hybrid of both hardwood and softwood to increase the dimensional stability of the panels while still providing higher bending stiffness values. As Figure 3 shows, the stiffest hybrid lay-up was found to be the panel with hardwood in the outer layers and softwood in the inner layers.

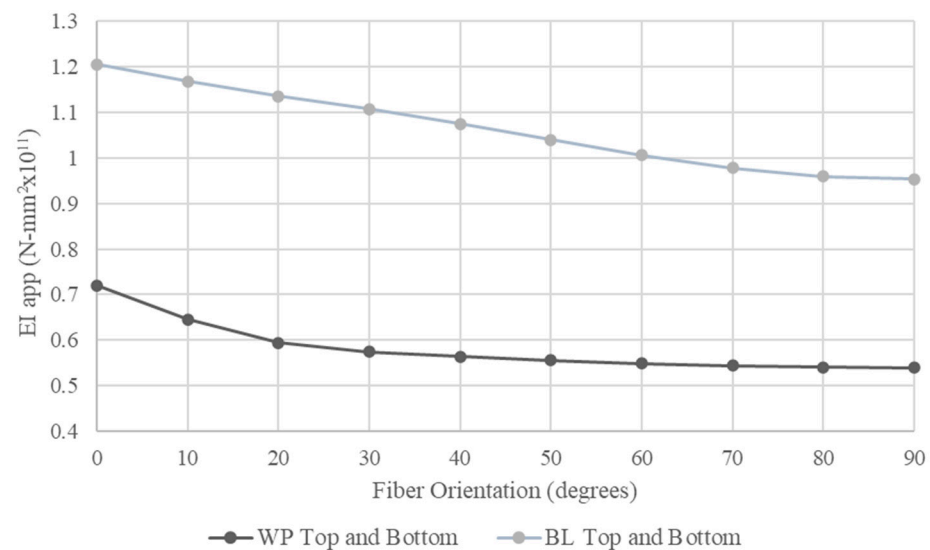


Figure 3. Apparent bending stiffness properties of two alternatives of hybrid DCLT panels with two species of white pine (WP) and black locust (BL).

2.2. DCLT Panel Preparation

A total of 1.8 m³ (750 board feet) of ungraded, rough-sawn, random width, 31 mm thickness, 3 m length black locust boards were purchased from a sawmill in Newfield, NY. Also, a total of 24 NeLMA [14] finish grade, flat-sawn, eastern white pine boards with 22 mm thickness, 197 mm width, and 3.65 m length were purchased from a local lumber yard near Syracuse, NY. The eastern white pine boards had been kiln-dried and surfaced on four sides (S4S), but the black locust boards needed to be conditioned and surfaced (S4S) before fabrication. All the boards were then placed in an ambient temperature

laboratory room to reach an equilibrium moisture content of approximately 12%. The average moisture content of the boards, determined with a Delmhorst (BD 2100) pin-type moisture meter, was measured as 11.8% at the time of fabricating the specimens. They were surfaced and planed to the desired thickness of 19 mm. Three replicates of each four-ply DCLT ($\pm 10^\circ$, $\pm 20^\circ$, $\pm 40^\circ$, and 70°) and one four-ply CLT (DCLT 90°) panel were fabricated to final dimensions of 76 mm thick, 30 cm wide, and 2.74 m long. Figure 4 illustrates the dimensions and the orientation of the panels. The width-to-thickness ratio of all the diagonal DCLT panels in this study followed the standard recommendations of 4:1 to limit the impact of rolling shear [15]. The white pine boards (angle plies) were cut to the desired size from straight grain and defect-free sections, eliminating the possible effects of knots on the results. However, because of the NeLMA finish grade's small knots and the difficult process of cutting the boards in different grain orientations, as shown in Figure 5a, minimal numbers of small knots were included in some of the boards. Before panel assembly, the longitudinal modulus of elasticity (MoE) of each black locust board (individual outer layer) and three eastern white pine sample boards was measured using the flatwise measured deflection of a simply supported board under a non-destructive center-point loading.

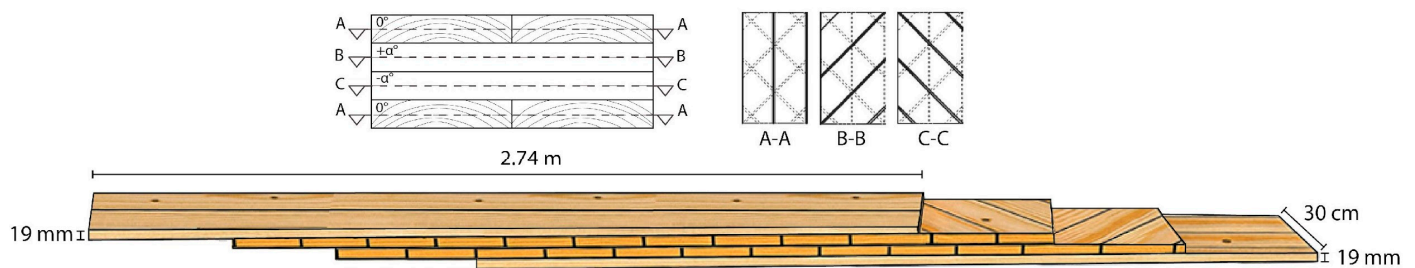


Figure 4. Dimensions and orientations of DCLT panels of the study.



Figure 5. From top left, (a) cutting of boards to desired grain orientation (representative sample at 10°), (b,c) DCLT panel's gluing process, and (d) DCLT panel's pressing process.

For panel fabrication, the boards were face-glued using Loctite HB X452 Purbond (Henkel Corporation, Bridgewater, NJ, USA) polyurethane adhesive with a recommended spread rate of 180 g/m^2 to glue the top and bottom of the lamina (face-glued) and without paying attention to the position of the board defects. The grain orientations of boards used in the inner layers were alternated in the second and third layers (Figure 4). The DCLT panels and the CLT panel clamping pressure was controlled by calibrated tightening torque set at 81.3 N.m (60 ft.lbf) per Equation (6) for torque-turn-tension control [16] to attain a minimum pressure of 410 kPa for 24 h, using a mechanical press and a pneumatic impact wrench.

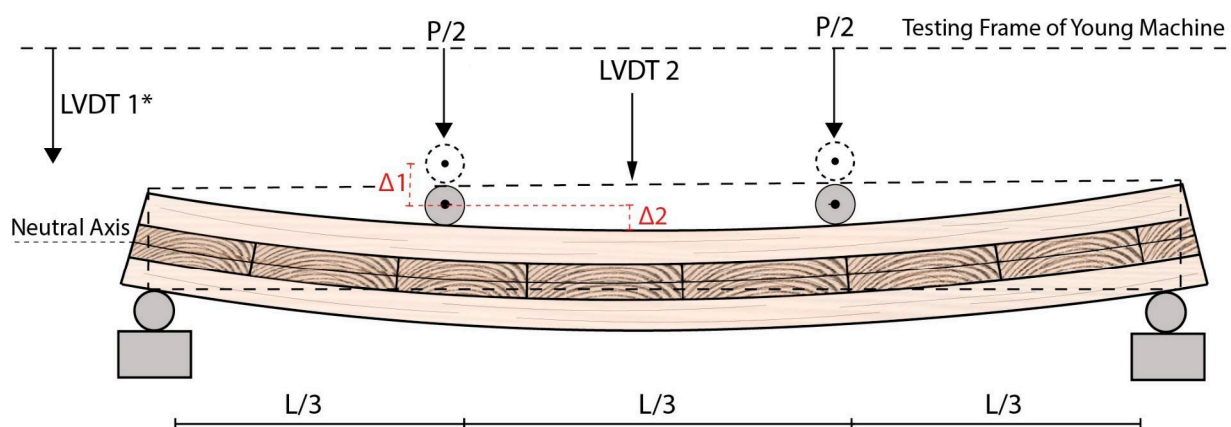
$$T = K \times D \times F \quad (6)$$

where T is the required torque energy, K is the nut factor (depending on characteristics of the nut), D is the nominal diameter, and F is the desired force value. The nut factor is a variable determined by the nut geometry, the friction in the threads, and the friction between the nut, washer(s), and sealing surface. In this case, friction values were initially assumed for the well-oiled interfaces, and the actual clamping force was confirmed by placing pressure-sensitive indicating film (Fujifilm Prescale[®] Sensor Products Inc. Madison, NJ, USA) between the pressing platen and the CLT beam face.

The torque was applied until a specified “threshold” level was attained and an additional angle-of-turn was applied to finish the installation. Figure 5a–d show the panels’ preparation process.

2.3. Four-Point Bending Test

Four-point load tests as outlined in ASTM D 198 [17] were performed on the panels using a Young universal testing machine outfitted with a 445 kN load cell with the crosshead speed of 0.001 mm/.min and two linear variable differential transducers (LVDTs). One LVDT was connected to the Young testing machine to measure the local displacement of load heads over a $0\text{--}150 \text{ mm}$ range, and the other one was installed on the top center of the panel to measure the displacement of the top center of the panel relative to the load heads over a $0\text{--}75 \text{ mm}$ range. The deflections from both LVDTs and loading data were recorded with LabView[®] Software (2020 Version) [18] on a dedicated personal computer. The total deflection was the sum of the two recorded deflections from LVDTs. The experimental setup is illustrated schematically in Figure 6 with the actual test set-up shown in Figure 7.



*LVDT 1 is mounted to the side of testing machine and is in contact with a fixed part of the testing frame.

Figure 6. Schematic representation of testing arrangement and LVDTs’ locations for DCLT bending specimens.



Figure 7. Actual testing arrangement for DCLT bending specimens.

The corresponding bending stiffness value from this test setup was acquired from Equation (7) ASTM D 198 [17]:

$$E_{app} = \frac{23 \times l^3}{108 \times b \times h^3} \times \frac{P}{\Delta} \quad (7)$$

where E_{app} is the apparent bending stiffness, P/Δ is the slope of the linear range of the load–deformation curve below the proportional limit with P and Δ accordingly being the maximum load and deflection at the proportional limit, l is the span length, and b and h are the width and the thickness of the specimen.

2.4. Finite Element Method

In order to further understand the bending performance of DCLT panels and the experimental results of the four-point test on the specimens, a numerical finite element (FE) model was developed using the research version of ANSYS Workbench 2022 [19] finite element software. The panels were modeled using two different linear elastic orthotropic element types, one for black locust in the top and bottom layers, and one for eastern white pine in the cross layers.

Nine independent elastic constants are required to define the mechanical response of an orthotropic material in the simulation. These constants are three elastic moduli (E), three Poisson's ratios (ν), and three shear moduli (G). For the material property values input in the simulations, the longitudinal elastic moduli values (E_L) for black locust and eastern white pine were obtained from the USDA Wood Handbook [20]. There are no available published values for the ratio of E_T/E_L , E_R/E_L , G_{TR}/E_L , G_{LR}/E_L , G_{TL}/E_L or the Poisson's ratios for the species used in this study.

The USDA Wood Handbook [20] provides elastic ratios with respect to the longitudinal elastic modulus for some softwood and hardwood species. However, there are no available published values or elastic ratios for the constants of E_R , G_{TL} , and E_T or the three required Poisson's ratios for eastern white pine. To predict these elastic constants using the available longitudinal (parallel to the grain) modulus of elasticity value, linear regressions (confidence level of 95%) were performed on each constant of the species in the USDA Wood Handbook [20] with available elastic ratios, regarding the longitudinal MoE as the predictor using Microsoft Excel [21]. The regressions showed R-squares ranging from 80% to 99% and a p -value less than the significance level (0.05) indicating a validation for prediction with a statistically significant correlation between the MoE and the response elastic constant [22].

The found ratios were repeated for another set of modeling considering the measured longitudinal MoE (from a simply supported bending test prior to panel fabrication) of black locust and eastern white pine boards as the longitudinal modulus of elasticity values. The final elastic constants for materials in FEM simulations are reported in Table 1.

Table 1. The ANSYS properties (black locust and eastern white pine) input for DCLT panels.

Species	Poisson's Ratio			Shear Modulus (MPa)			Young's Modulus (MPa)			Specific Gravity
	ν_{lt}	ν_{lr}	ν_{tr}	G_{lr}	G_{lt}	G_{rt}	E_t	E_r	E_l	
Black locust (Wood Handbook MoE)	0.286	0.220	0.196	1301	899	274	862	1697	14,134	0.69
Eastern white pine (Wood Handbook MoE)	0.233	0.223	0.220	624	592	76	467	766	8549	0.35
Black locust (Measured MoE)	0.286	0.220	0.196	1587	1096	334	1051	2070	17,236	0.69
Eastern white pine (Measured MoE)	0.233	0.223	0.220	548	520	67	411	673	7515	0.35

FEM ANSYS Workbench [19] simulations were performed under the “Static Structural” analysis system on one model of each DCLT $\pm 10^\circ$, DCLT $\pm 20^\circ$, DCLT $\pm 40^\circ$, DCLT $\pm 70^\circ$, and CLT specimens. The panels were modeled with the specifications for material, loading, and boundary conditions as shown in Figure 8 identical to the experimental four-point bending test to assure the accuracy of the comparison and validation.

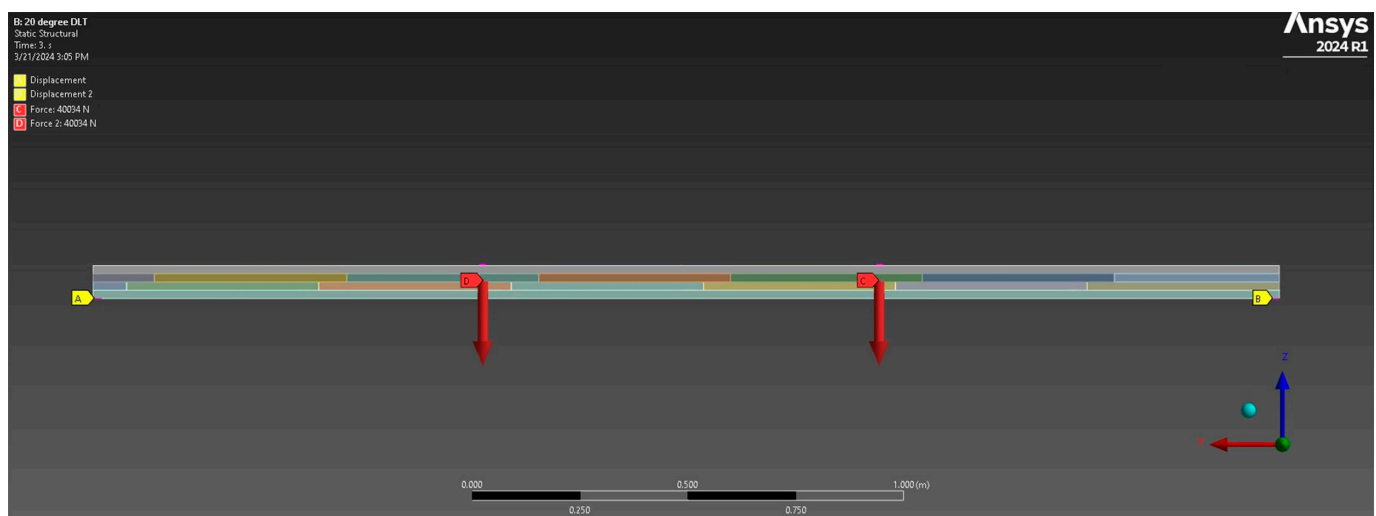


Figure 8. FEM modeling boundary condition for four-point bending test.

Mesh refinement as shown in Figure 9 was also performed under mechanical physics preference (program-controlled element order) by subdividing the mesh size to the rectangular elements with the size of 7 mm for each solid geometry. The mesh elements used for the sample specimens were higher order elements: SOLID186 element: 3D 20 nodes, TARGE170 3D target surface for the associated contact element of CONTA174: 3D 8 nodes surface-to-surface, and SURF154: 3D structural surface effect. Table 2 shows the details of the mesh sizing and the refinement quality of the model.

For each set of simulations, three coordinate systems were defined regarding the parallel (0° , global coordinate system) and two diagonal layers with $\pm\alpha^\circ$ rotation of the main axis direction (x-y). The simulation's details and the details of different coordinate systems designed in the modeling are shown in Figure 10. After each simulation, load–

deflection data were recorded to calculate the bending stiffness of each sample using Equation (7).

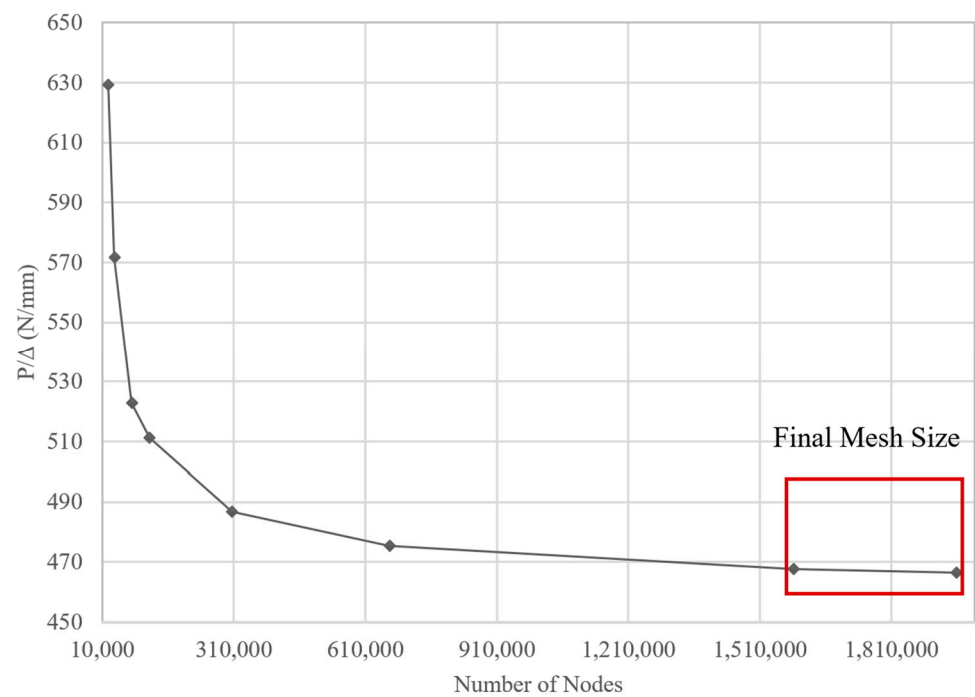


Figure 9. Mesh convergence for one DCLT representative sample.

Table 2. Mesh sizing and details for ANSYS modeling.

Group	Bounding Box Diagonal Size (cm)	Average Surface Area (cm ²)	Minimum Edge Length Size (cm)	Number of Nodes	Number of Elements
DCLT ± 10	276.93	803.67	0.96	2,111,626	413,142
DCLT ± 20	276.93	584.96	0.12	1,983,392	387,159
DCLT ± 40	277.08	383.61	0.43	1,466,501	283,758
DCLT ± 70	276.93	322.12	1.90	388,696	66,528
CLT	276.93	307.03	1.90	913,030	174,240

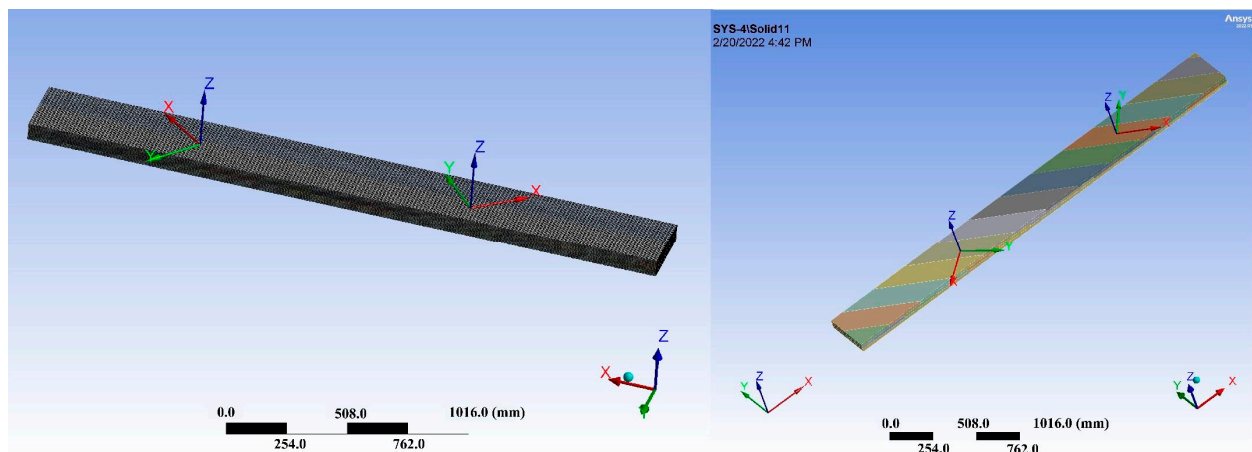


Figure 10. Representative samples of the finite element meshing and modeling showing details of relative mesh size and coordinate systems.

3. Results and Discussion

3.1. Hankinson's Theory Results

To evaluate the bending stiffness of the DCLT panels, the apparent bending stiffness has been calculated using the shear analogy approach. As mentioned in the Methodology section, Hankinson's equation has been used in the shear analogy approach to provide the stiffness properties of the angled inner layers of the panels.

Table 3 provides a summary of the bending stiffness values predicted by the shear analogy approach and the percent increase from each increment. Values for the theory use both the assumed MoE (i.e., USDA Wood Handbook [20]) and the measured MoE of the outer layers.

Table 3. Bending stiffness properties for different grain orientations obtained from Hankinson's theory.

EI_{App} ($N\text{-mm}^2 \times 10^{11}$)	Grain Orientation				
	10°	20°	40°	70°	90°
Handbook Values	1.45	1.39	1.31	1.21	1.18
MoE of the Layers	1.74	1.68	1.58	1.43	1.40
% Increase to CLT	23%	18%	12%	3%	--

3.2. Four-Point Bending Test Results

As shown in Figure 11, the slope of the load–deflection curves decreases, while the angle-ply orientation increases toward 90° or CLT. Therefore, the grain orientation of the inner layers is confirmed to affect the stiffness of the panels. Regarding the data from the testing shown in Table 4, the apparent bending stiffness of the panels is improved by 33% from CLT to DCLT $\pm 10^\circ$. This indicates that grain orientation had a statistically significant (p -value of 0.009) effect on the apparent bending stiffness of the DCLT panels. Table 4 also summarizes the difference percentages (%) between the bending stiffness properties of DCLT panels with different grain orientations in inner layers.

Table 4. Bending stiffness properties for different grain orientations obtained from experimental tests.

$EI_{App.}$ ($N\text{-mm}^2 \times 10^{11}$)	Grain Orientation				
	10°	20°	40°	70°	90°
Mean	2.28	2.14	1.95	1.76	1.71
% Increase to CLT	33%	25%	14%	3%	--
COV (%)	2.62	5.93	3.37	7.42	--
Min	2.23	2.00	1.90	1.67	1.71
Max	2.35	2.26	2.02	1.91	1.71

The beams were loaded to failure, and the first cracks started to form outside of the center third and closer to the ends due to rolling shear failure. This region provides the low secondary stresses originating from load heads or bearing supports, and with increasing load, the deformation propagates along the length of the panel toward the supports, where eventually the combination of the shear and bending stresses resulted in the final fracture.

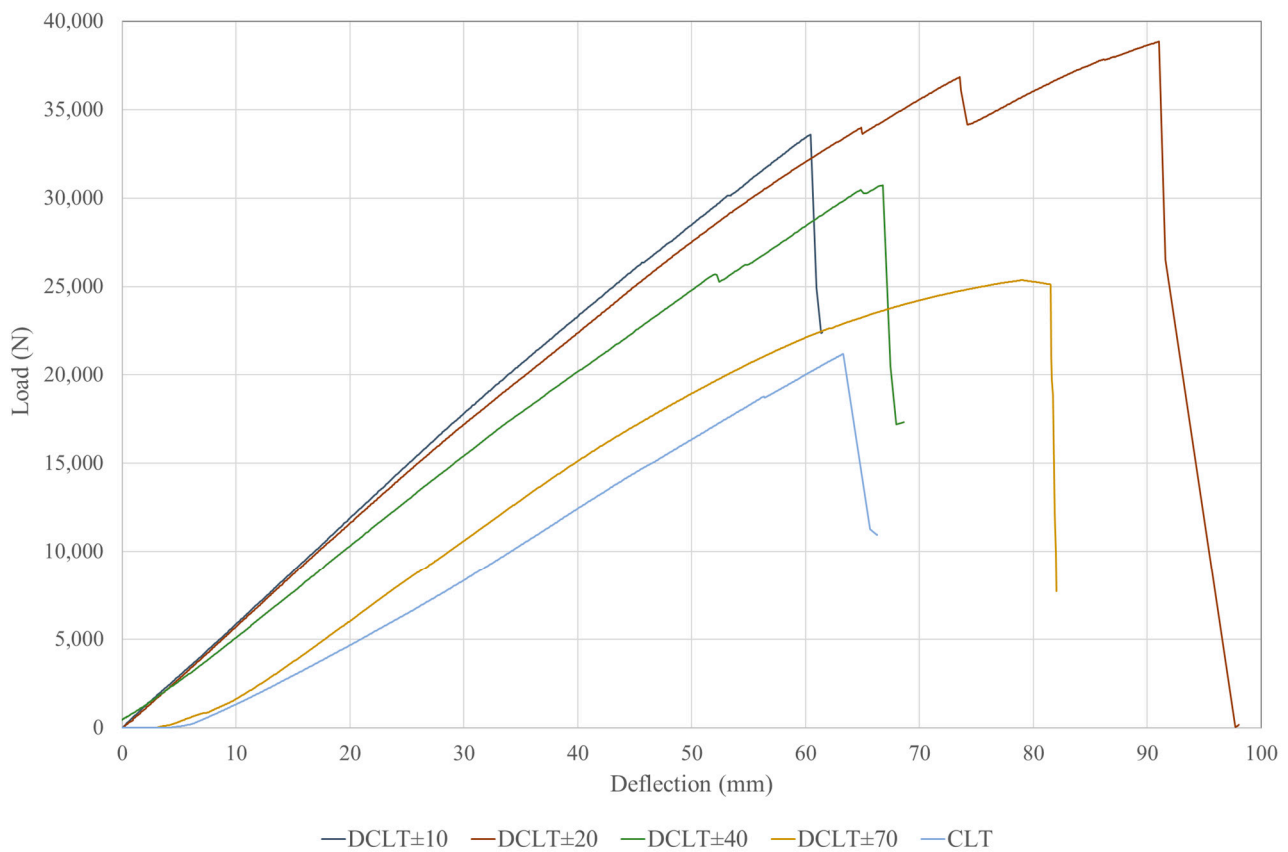


Figure 11. Load–deflection curves of DCLT $\pm \alpha$ representative samples tested under four-point bending tests.

3.3. Finite Element Analysis

After each DCLT $\pm \alpha$ sample was tested under the simulations, the deflection results from the four-point bending loading were recorded. As shown in Figure 12, the maximum deflection occurs in the center of the panel between the two loading areas. To demonstrate this process, the load–deflection curve for each sample model was recorded as shown in Figure 13, and slopes of the curves were used for measuring the bending stiffness of DCLT panels.

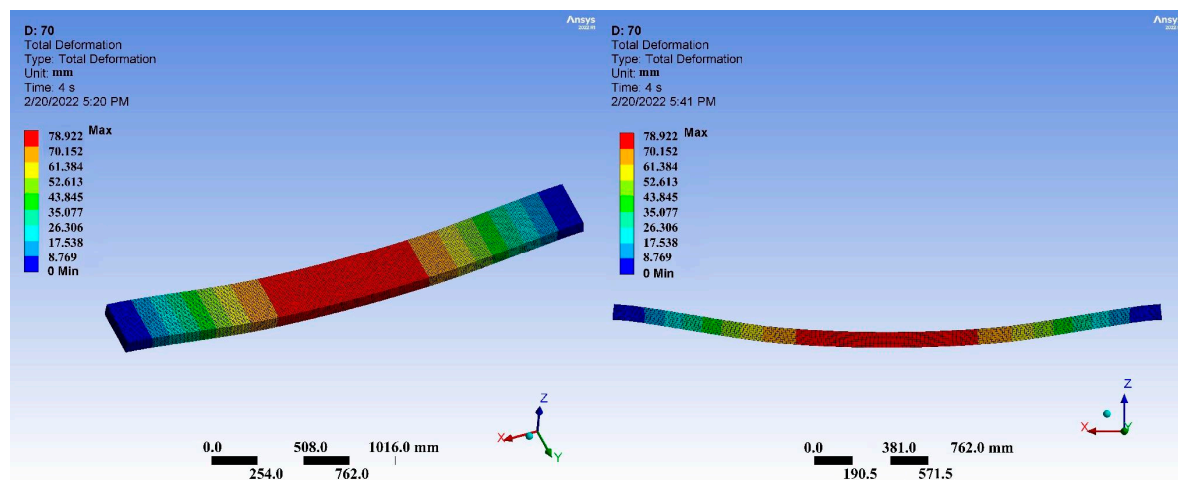


Figure 12. FEM test deflection results for a DCLT sample under applied load.

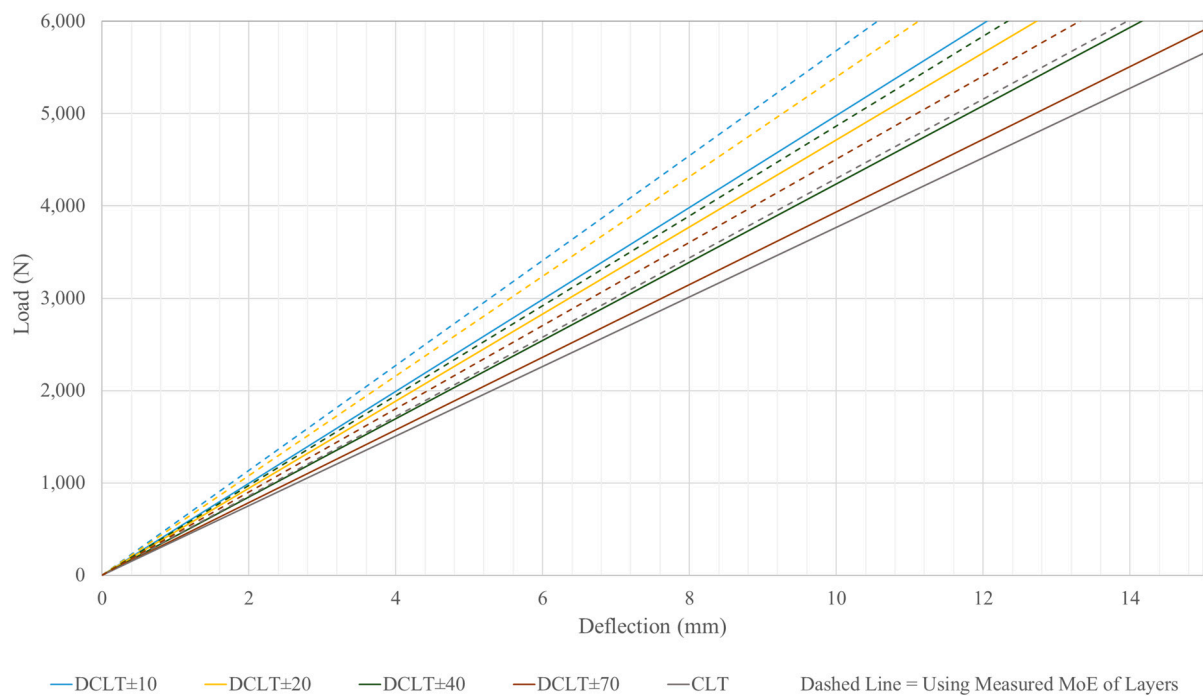


Figure 13. Load–deflection curves of DCLT $\pm \alpha$ samples from FEM simulations.

The simulations were repeated one more time with the material properties of black locust and eastern white pine being considered with the measured MoE value instead of the published handbook values. As the results show, the simulated DCLT samples with the measured MoE have approximately 12–14% higher apparent bending stiffness than the results using the published E_L .

Regarding the data presented in Table 5, the FEM validates the experimental and theoretical results indicating that decreasing the angle of the grain orientation in the inner layers of the panels increases the bending stiffness. The finite element method data show that DCLT $\pm 10^\circ$ has an improved apparent bending stiffness by approximately 35% (compared to 90° lay-up) when using either the USDA Wood Handbook [20] values or the measured MoE of the outer layers as the input for simulated models. Table 5 also summarizes the percent difference (%) between the bending stiffness properties of DCLT panels with different grain orientations in inner layers.

Table 5. Bending stiffness properties for different grain orientations obtained from FEM simulations.

EI_{App} ($N \cdot mm^2 \times 10^{11}$)	Grain Orientation				
	10°	20°	40°	70°	90°
Handbook Values	1.94	1.85	1.65	1.53	1.46
MoE of the Layers	2.32	2.18	1.96	1.81	1.72
% Increase to CLT	33%	26%	13%	6%	--

3.4. DCLT's Bending Stiffness Comparison between the Methods

Considering all the assessed methods in this study, Figure 14 shows the final apparent bending stiffness results of each method for comparison. All the methods confirmed that decreasing the angle of the grain orientation in the inner layers of the panels increases the bending stiffness. This is due to the fact that by decreasing the inner lamina grain orientation, these layers will no longer be stressed under shear perpendicular to the grain but parallel to the grain (which is higher than shear perpendicular to the grain), which means the specimen then shows a higher bending stiffness. As the plots indicate, the

highest values for all the grain orientations of DCLT panels and the CLT panel are from the results of FEM modeling using the measured MoE of the boards. This FEM result is very similar to the experimental results from four-point bending tests due to higher and more accurate elastic constant values as (or for) the material properties input. An obvious observation is that using the measured MoE of the layers provides more accurate models than using the reference MoE from the Wood Handbook when used in either numerical or theoretical modeling. The results from the theory (Hankinson's formula in shear analogy) under-predict the apparent bending stiffness. The results from these experiments show approximately 50% higher values of apparent bending stiffness compared to the theoretical values from the Hankinson/shear analogy approach with the published USDA Wood Handbook reference values, which makes this method of prediction a conservative model requiring further investigations to provide a more accurate analytical model.

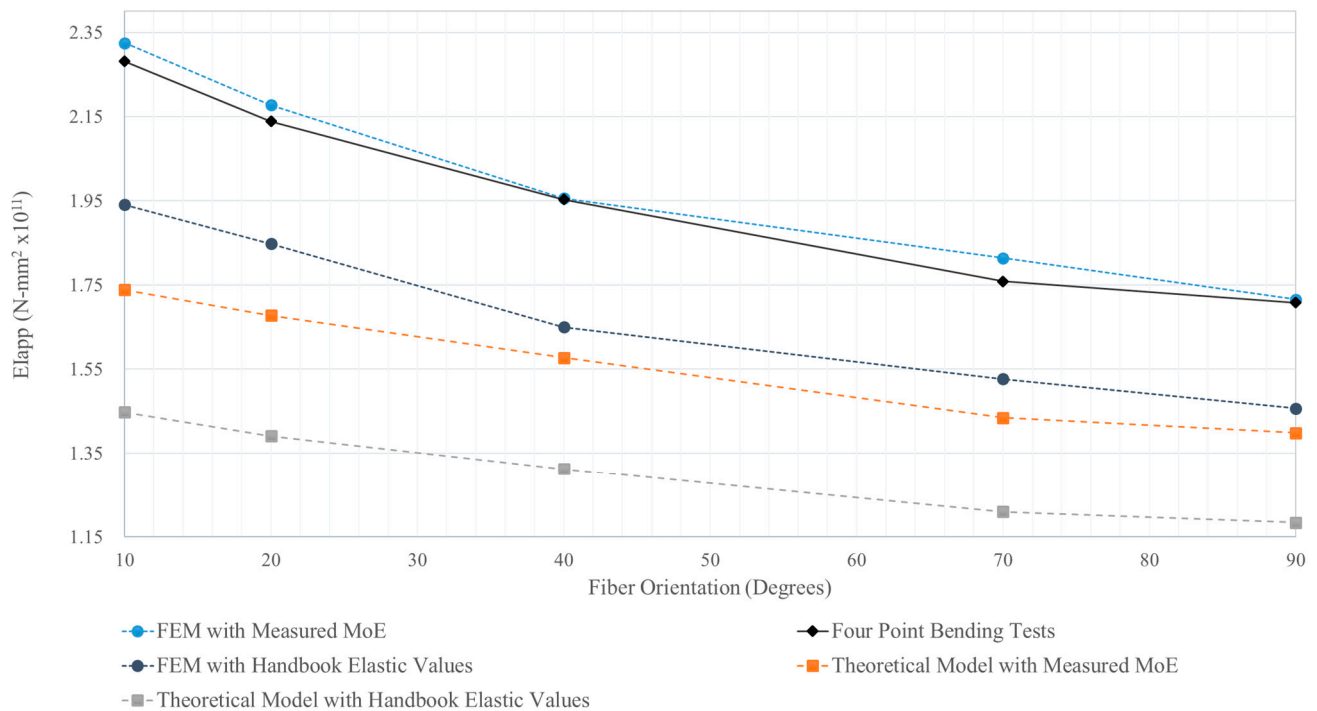


Figure 14. Apparent bending stiffness of DCLT/CLT panels predicted from four different methods.

This study is also in agreement with the previous literature on DCLT's structural advantages compared to conventional CLT. The current study shows an increase of 14% for the apparent bending stiffness from CLT to DCLT $\pm 40^\circ$, which is very similar to results from four-point bending tests on DCLT $\pm 45^\circ$ panels conducted by Buck et al. [4], which showed an increase of 15% in the El_{app} from CLT. However, the apparent bending stiffness increases from CLT to 30° (174%), 45° (112%), and 60° (61%) in Bahmanzad et al. [5]'s study, which was conducted using a short-span three-point bending test, which appears to be significantly different from what might be concluded to be the testing fixture and its application for measuring the shear stiffness rather than bending stiffness.

4. Conclusions

This study investigated the bending stiffness of four-ply Diagonal-Cross-laminated Timber (DCLT) panels consisting of five different grain orientations of 90° (CLT), 70° , 40° , 20° , and 10° in the cross layers. According to the four-point bending tests, the DCLT $\pm 10^\circ$ panels were the stiffest followed successively by the DCLT $\pm 20^\circ$, $\pm 40^\circ$, $\pm 70^\circ$, and 90° (CLT) panels. These results support the modeled results acquired from Hankinson's input in shear analogy and FEM simulations. The results from the three methods agreed that the decrease in the angle of the inner layer grain reorientation would improve the bending

stiffness properties of CLT panels. The apparent bending stiffness from DCLT 90° to DCLT $\pm 10^\circ$ has an increase of 33%, 24%, and 35%, respectively, regarding the assessed methods of experimental, theoretical, and FEM modeling. This study indicates that DCLT panels with angle-ply cross layers have a structural advantage over traditional CLT (90°) panels. This study could be further expanded for investigation on other inner lamina orientations of DCLT products to propose an optimized grain orientation considering the structural and dimensional integrity of GLT and CLT. Using these panels would allow for increased spans or load-carrying capacity for a given panel span-to-depth ratio. The development of DCLT and its introduction to the industry could also enable the utilization of lower-quality timber that would not otherwise satisfy structural requirements for CLT. DCLT opens new possibilities for efficient material usage in massive timber construction. Additionally, this study validates methods of predicting the bending stiffness of DCLT and CLT panels with the available or measured elastic modulus parallel to the grain of the species used in the panel fabrication. This method of prediction could help utilize and introduce non-standard species for the fabrication of these products.

Author Contributions: Conceptualization, P.L.C.; Methodology, S.K.; Software, S.K.; Validation, P.L.C.; Formal analysis, S.K.; Investigation, S.K.; Resources, P.L.C.; Data curation, S.K.; Writing—original draft, S.K.; Writing—review & editing, P.L.C.; Visualization, S.K.; Supervision, P.L.C.; Project administration, P.L.C.; Funding acquisition, P.L.C. All authors have read and agreed to the published version of the manuscript.

Funding: This research was generously supported by a USDA Wood Innovation Grant, grant number: 20-DG-11094200-179.

Institutional Review Board Statement: Not applicable.

Informed Consent Statement: Not applicable.

Data Availability Statement: The data presented in this study are available in the article.

Conflicts of Interest: The authors declare no conflict of interest.

References

1. Bejtka, I. *Cross (CLT) and Diagonal (DLT) Laminated Timber as Innovative Material for Beam Elements*; Karlsruher Institut für Technologie (KIT) Scientific Publishing: Karlsruhe, Germany, 2011.
2. Arnold, M.; Dietsch, P.; Maderebner, R.; Winter, S. Diagonal laminated timber: Experimental; analytical, and numerical studies on the torsional stiffness. *Constr. Build. Mater.* **2022**, *322*, 126455. [\[CrossRef\]](#)
3. Kurzinski, S.; Crovella, P.; Smith, W. Evaluating the Effect of Inner Layer Grain Orientation on Dimensional Stability in Hybrid Species Cross-and Diagonal-Cross-laminated Timber (DCLT). *Mass Timber Constr. J.* **2023**, *6*, 11–16.
4. Buck, D.; Wang, X.A.; Hagman, O.; Gustafsson, A. Bending properties of Cross Laminated Timber (CLT) with a 45° alternating layer configuration. *BioResources* **2016**, *11*, 4633–4644. [\[CrossRef\]](#)
5. Buck, D.; Hagman, O. Mechanics of Diagonally Layered Cross-laminated Timber. In Proceedings of the World Conference on Timber Engineering WCTE 2018, Seoul, Republic of Korea, 20–23 August 2018.
6. Bahmanzad, A.; Clouston, P.L.; Arwade, S.R.; Schreyer, A.C. Shear Properties of Symmetric Angle-Ply Cross-Laminated Timber Panels. *J. Mater. Civ. Eng.* **2020**, *32*. [\[CrossRef\]](#)
7. Yoshito, M.; Hiroe, K.; Yukari, T.; Yasue, N. Relationship between the Strength and Grain Orientation of Wood: Examination and modification of the Hankinson's Formula. *Univ. Tokyo Grad. Sch. Agric. Life Sci. Exerc. Forest.* **1995**, *93*, 1–5.
8. Bahmanzad, A.; Clouston, P.L.; Arwade, S.R.; Schreyer, A.C. Shear Properties of Eastern Hemlock with Respect to Fiber Orientation for Use in Cross Laminated Timber. *J. Mater. Civ. Eng.* **2020**, *32*, 04020165. [\[CrossRef\]](#)
9. Franzoni, L.; Lebé, A.; Lyon, F.; Foret, G. Influence of orientation and number of layers on the elastic response and failure modes on CLT floors: Modeling and parameter studies. *Eur. J. Wood Wood Products.* **2016**, *74*, 671–684. [\[CrossRef\]](#)
10. Kreuzinger, H. Platten, Scheiben und Schalen. **1999**, *101*, 34–39. (In German)
11. Karacebeyli, E.; Douglas, B. *CLT Handbook—US Edition*; FPinnovations and Binational Softwood Lumber Council: Point-Claire, QC, Canada, 2013.
12. Kurzinski, S.; Crovella, P.L. Predicting the Strength and Serviceability Performance of Cross-Laminated Timber (CLT) Panels Fabricated with High-Density Hardwood. In Proceedings of the World Conference on Timber Engineering, WCTE 2021, Santiago, Chile, 9–12 August 2021.
13. American Wood Council's (AWC) Wood Design Standards Committee. *National Design Specification (NDS) for Wood Construction*; AWC: Leesburg, VA, USA, 2018.

14. American Lumber Standard Committee (ALSC). *Northeastern Lumber Manufacturers Association, Standard Grading Rules for Northeastern Lumber*; Northeastern Lumber Manufacturers Association: Cumberland Center, ME, USA, 2021.
15. ANSI-APA/PRG 320; Standard for Performance-Rated Cross-Laminated Timber. American National Standard Institute & APA—The Engineered Wood Association: New York, NY, USA, 2019.
16. Shoberg, R.S. *Engineering Fundamentals of Threaded Fastener Design and Analysis*; RS Technologies, a Division of PCB Load & Torque, Inc., 2000; pp. 1–39. Available online: <http://www.hexagon.de/rs/engineeringfundamentals.pdf> (accessed on 5 March 2024).
17. ASTM D 198-15; Standard Test Methods of Static Tests of Lumber in Structural Sizes. American Society for Testing and Materials Committee: West Conshohocken, PA, USA, 2015.
18. National Instruments Corporation. *Software Recording the Test*; LabVIEW 2020 Version: Austin, TX, USA, 2021.
19. ANSYS Inc. *ANSYS®Workbench*; ANSYS Inc.: Canonsburg, PA, USA, 2022.
20. Forest Products Laboratory. *USDA Wood Handbook—Wood as an Engineering Material*; General Technical Report FPL-GTR-190; Forest Products Laboratory: Madison, WI, USA, 2021. [[CrossRef](#)]
21. Microsoft Corporation. *Microsoft Excel*; Microsoft Corporation: Redmond, WA, USA, 2021.
22. Kurzinski, S.; Crovella, P.L. Theoretical and Experimental Investigation on Predicting Longitudinal and Tangential Elastic Constants and Ratios of Wood. In Proceedings of the World Conference on Timber Engineering, WCTE 2023, Oslo, Norway, 19–22 June 2023. [[CrossRef](#)]

Disclaimer/Publisher’s Note: The statements, opinions and data contained in all publications are solely those of the individual author(s) and contributor(s) and not of MDPI and/or the editor(s). MDPI and/or the editor(s) disclaim responsibility for any injury to people or property resulting from any ideas, methods, instructions or products referred to in the content.